Cyclooxygenase-2 Inhibits Novel Ginseng Metabolite-Mediated Apoptosis

Hyung Woo Yim,[1] Hyun-Soon Jong,[1] Tai Young Kim,[1] Hyun Ho Choi,[1] Sang Gyun Kim,[1] Sang Hyun Song,[1] Juyong Kim,[1] Seong-Gyu Ko,[1] Jung Weon Lee,[1] Tae-You Kim,[1,2] and Yung-Jue Bang[1,2]

[1]National Research Laboratory for Cancer Epigenetics, Cancer Research Institute and [2]Department of Internal Medicine, Seoul National University College of Medicine, Chongno, Seoul, Republic of Korea

Abstract

Recently, a novel intestinal bacterial metabolite of ginseng protopanaxadiol saponins, i.e., 20-*O*-(β-D-glucopyranosyl)-20(*S*)-protopanaxadiol (IH-901), has been reported to induce apoptosis in a variety of cancer cells. Here we show a differential effect of IH-901 on several cell types. Exposure to IH-901 for 48 hours at a supposedly subapoptotic concentration of 40 μmol/L led to both apoptotic cell death and G_1 arrest in Hep3B cells, but only resulted in G_1 arrest in MDA-MB-231, Hs578T, and MKN28 cells. Additionally, the treatment of MDA-MB-231, but not of Hep3B, with IH-901 up-regulated cyclooxygenase-2 (COX-2) mRNA (2 hours) and protein (6 hours), and enhanced the production of prostaglandin E_2. In MDA-MB-231 cells, IH-901 induced the sustained activation of extracellular signal-regulated kinase (ERK), whereas inhibition of mitogen-activated protein/ERK kinase blocked IH-901-mediated COX-2 induction and resulted in apoptosis, suggesting the involvement of an ERK-COX-2 pathway. Combined treatment with IH-901 and nonsteroidal anti-inflammatory drugs inhibited COX-2 enzyme and induced apoptosis in MDA-MB-231 and Hs578T cells. Adenovirus-mediated COX-2 small interfering RNAs also effectively inhibited COX-2 protein expression and enhanced IH-901–mediated apoptosis without inhibiting ERK 1/2 phosphorylation, thus providing direct evidence that COX-2 is an antiapoptotic molecule. Moreover, IH-901–mediated G_1 arrest resulted from an increase in $p27^{Kip1}$ mRNA and protein expression followed by a decrease in CDK2 kinase activity that was concurrent with the hypophosphorylation of Rb and p130. In conclusion, IH-901 induced both G_1 arrest and apoptosis, and this apoptosis could be inhibited by COX-2 induction. (Cancer Res 2005; 65(5): 1952-60)

Introduction

Panax ginseng C.A. Meyer is an herbal root that has been used for more than 2000 years throughout Far Eastern countries including China, Japan, and Korea. Its beneficial effects have been analyzed by extensive preclinical and epidemiological studies (1–3). Recently, 20-*O*-(β-D-glucopyranosyl)-20(*S*)-protopanaxadiol (IH-901), a novel ginseng saponin metabolite, formed from ginsenosides Rb1, Rb2, and Rc was isolated and purified after giving ginseng extract p.o. to humans and rats (4). IH-901 has been shown to enhance the efficacy of anticancer drugs in cancer cell lines previously resistant to several anticancer drugs (5, 6), to exhibit antigenotoxic and anticlastogenic activity in rats concurrently treated with benzo(*a*)pyrene (7), and to induce apoptosis (8, 9). These studies found that the antitumor activity of IH-901 is attributable to the induction of apoptosis.

Recently, the link between cyclooxygenase (COX)-2 and cancer has been studied (10, 11). COX catalyzes the conversion of arachidonic acid to prostaglandins and related eicosanoids. Two isoforms of COX, which are the products of distinct genes, have been identified. COX-2 is an inducible and immediate-early gene that is up-regulated in many epithelial malignancies (12–15). Unlike constitutively expressed COX-1, COX-2 overexpression is associated with neoplastic transformation (12), cell growth (16), angiogenesis (17), invasiveness, and metastasis (18). Although *in vivo*, the exact mechanism has not been clearly elucidated, *in vitro* studies have shown in a variety of cell types that COX-2 overexpression is antiapoptotic (19). This antiapoptotic effect is associated with inhibition of Fas (20) and up-regulation of Bcl-2 (21). Even though COX-2 is an important target for cancer therapy, COX-2 is induced by several anticancer agents such as paclitaxel (22), mitomycin C (23), and radiation (24), suggesting its association with drug resistance.

Physiologically, $p27^{Kip1}$ seems to be important for blocking progression of cells from late G_1 into S via its interaction with cyclin E-CDK2 complexes (25). $p27^{Kip1}$ has been also implicated as a mediator of the growth arrest due to its regulation by protein kinase A activating agents (26). IH-901 stimulated $p27^{Kip1}$ induction and subsequent cell cycle (G_1) arrest.

In this study, we discovered that IH-901, a novel ginseng metabolite, could inhibit human cancer cell proliferation by inducing cell cycle arrest as well as apoptosis. Treatment with IH-901 resulted in cell cycle (G_1) arrest by $p27^{Kip1}$ induction. Additionally, we provide evidence here that COX-2 functions as an antiapoptotic molecule as its inhibition by both nonsteroidal anti-inflammatory drugs (NSAID) and adenoviral-COX-2 small interfering RNAs (siRNA) significantly enhanced IH-901-mediated apoptosis. These findings provide a molecular basis for the antineoplastic effects of IH-901 and use of this ginseng metabolite may aid in enhancing the anticancer drug efficacy by COX-2 inhibition.

Materials and Methods

Reagents. IH-901 was kindly provided by Dr. J-H. Sung (Central Research Institute, Il Hwa Co., Ltd., Korea) and was previously described (9). NS-398 was purchased from Cayman Chemicals (Ann Arbor, MI); actinomycin D from Sigma Chemical Co. (St. Louis, MO); CDK2 (M2), cyclin E (C-19), Bax

Requests for reprints: Yung-Jue Bang or Hyun-Soon Jong, Cancer Research Institute, Seoul National University College of Medicine, 28 Yongon-Dong, Chongno-Ko, Seoul 110-744, Republic of Korea. Phone: 82-2-2072-2390; Fax: 82-2-2072-9662; E-mail: bangyj@plaza.snu.ac.kr or hsjong@snu.ac.kr.

and COX-2 antibodies from Santa Cruz Biotechnology (Santa Cruz, CA); $p21^{WAF1/CIP1}$ (C24420) and $p27^{Kip1}$ (K25020) antibodies from Transduction Laboratories (Lexington, KY); pRB (G3-245) antibodies from PharMingen (San Diego, CA); and Bcl-2 antibodies from DAKO (Denmark).

Cell Cultures. MDA-MB-231, Hep3B, and MKN28 cells were grown in RPMI 1640 supplemented with 10% heat-inactivated fetal bovine serum and gentamicin (10 μg/mL). Hs578T cell line was grown in DMEM supplemented with 10% fetal bovine serum, and gentamicin. Subconfluent monolayers of cells were utilized in all experiments.

3-(4,5-Dimethylthiazol-2-yl)-2,5-Diphenyltetrazoliumbromide Assay. Cell viability was determined by measuring the absorbance of 3-(4,5-dimethylthiazol-2-yl)-2,5-diphenyltetrazoliumbromide (Sigma) dye for living cells, as described earlier (9). IC_{50}'s were calculated based on the survival rate of untreated cells being 100%.

Cell Cycle Analysis. Apoptosis was monitored by measuring hypodiploid DNA content (sub-G_1). Cells (5×10^5) were seeded in 60 mm dishes and allowed to attach overnight. Cell cultures were then incubated with IH-901 at 40 μmol/L concentration for the indicated times. fluorescence-activated cell sorting analysis using propidium iodide (PI) was done as described previously (27). The relative DNA content per cell was obtained by measuring the fluorescence of DNA bound propidium iodide. Cell cycle analysis was conducted using a FACStar flow cytometer (Becton Dickinson, San Jose, CA) and a ModFit LT V2.0 computer program.

Chromosomal DNA Isolation and Ladder Formation Assay. Cells were harvested and then suspended in a lysis buffer [50 mmol Tris-Cl (pH 8.0), 10 mmol EDTA, and 0.5% laurylsarcosine] containing 50 μg/mL RNase A. Chromosomal DNA was isolated and ladder formation assays were done as described previously (9).

RNA Extraction, Northern Blot Analysis, and mRNA Stability Assay. Total RNA preparation and Northern blotting were done as described previously (28). Blots were hybridized with radiolabeled probes for COX-2 cDNA (kindly provided by Dr. Stephan M. Prescott, University of Utah) and a $p27^{Kip1}$ cDNA fragment for RNA expression. For mRNA stability assay, the relative band intensities of *$p27^{Kip1}$* and β-actin mRNA at each time point were quantified by determining radioactivity using a Fuji FLA2000 and image analysis software (Image Gauge, version 3.12).

Western Blot Analysis. Cells were washed with ice-cold PBS and suspended in lysis buffer [20 mmol Tris-Cl (pH 7.4), 100 mmol NaCl, 1% NP40, 0.5% sodium deoxycholate, 5 mmol $MgCl_2$, 0.1 mmol phenylmethylsulfonyl fluoride, 0.1 mmol pepstatin A, 0.1 mmol antipain, 0.1 mmol chymostatin, 0.2 mmol leupeptin, 10 μg/mL aprotinin, 0.5 mg/mL soybean trypsin inhibitor, and 1 mmol benzamidine] on ice for 30 minutes. Lysates were cleared by centrifugation at 13,000 rpm for 20 minutes. Equal amounts of cell extracts (100 μg) were resolved by SDS-PAGE, transferred to nitrocellulose membranes, and probed with appropriate primary and horseradish-conjugated secondary antibodies, as described previously (29). Anti-α-tubulin antibody (Sigma) was used as a loading control. Detection was done using an enhanced chemiluminescence system (Amersham Pharmacia Biotech, Buckinghamshire, United Kingdom).

Prostaglandin E_2 Production and Determination of COX-2 Activity. Cells were treated with IH-901 and/or celecoxib, a specific COX-2 inhibitor, for 24 hours in complete growth medium containing 10% fetal bovine serum. Afterwards, culture medium was collected to determine the amount of prostaglandin E_2 (PGE_2) secreted by the cells. For the measurement of COX-2 enzymatic activity, PGE_2 quantification was measured using a PGE_2 enzyme immunoassay kit (Cayman) according to the manufacturer's instructions, as described previously (30). Results are expressed as picograms of PGE_2 per 10^6 cell ± SD.

Immunoprecipitation and Kinase Assays. CDK2 and cyclin E-associated H1 histone kinase activity were determined as described previously (27). Two hundred micrograms of cell extracts were used per immunoprecipitation with CDK2 antibody coupled to protein A or G beads. After being washed, CDK2 kinase assays on histone H1 was done by incubating the immune complex beads with 30 μL of kinase reaction [0.25 μL (2.5 μg) of histone H1, 0.5 μL (5 μCi) of γ-[^{32}P]ATP, 0.5 μL of 0.1 mmol ATP and 28.75 μL of kinase buffer] for 30 minutes at 37°C. The reaction was stopped by boiling the samples in 2× SDS sample buffer for 5 minutes. Samples were analyzed by 12% SDS-PAGE, and the gels were then dried and subjected to autoradiography. Preimmune serum was also analyzed for possible nonspecific immunoprecipitation in these studies.

Construction of Recombinant Adenoviral Vector of siRNAs for COX-2 Gene. pSUPER vector (31) enabled us to directly clone synthetic oligonucleotides yielding U1 promoter–based knock-down constructs. Target sequences of the siRNA specific for COX-2 and GFP duplex are as follows: siRNA-COX-2#1 (M90100), 5′-AAC CGA GGT GTA TGT ATG AGT GT-3′; siRNA-COX-2#2, 5′-AAT GCA ATT ATG AGT TAT GTG TT-3′; and siRNA-pEGFP (U57609), 5′-GGC TAC GTC CAG GAG CGC ACC-3′. Both

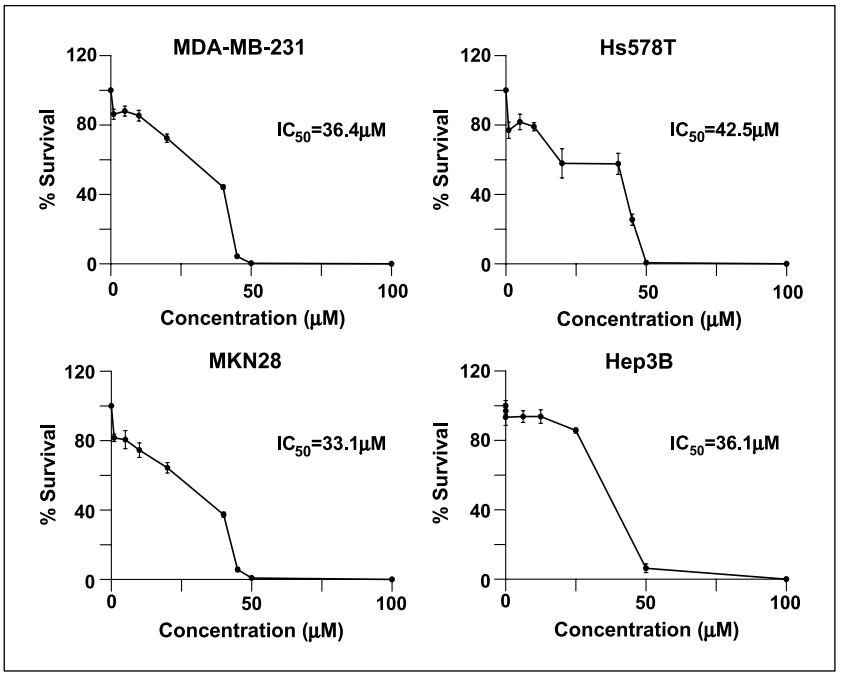

Figure 1. Growth inhibitory effects of IH-901 on MDA-MB-231 and Hs578T breast cancer cells, MKN28 gastric cancer cells, and Hep3B hepatocellular carcinoma cells. Exponentially growing cells were treated with the indicated concentration of IH-901 for 72 hours. Cell growth inhibition was analyzed by 3-(4,5-dimethylthiazol-2-yl)-2, 5-diphenyltetrazoliumbromide assay, as described in Materials and Methods. *Inset,* IC_{50} values of the individual cell lines. The assay was done using six replicates and repeated more than thrice. *Points,* mean; *bars,* ± SE.

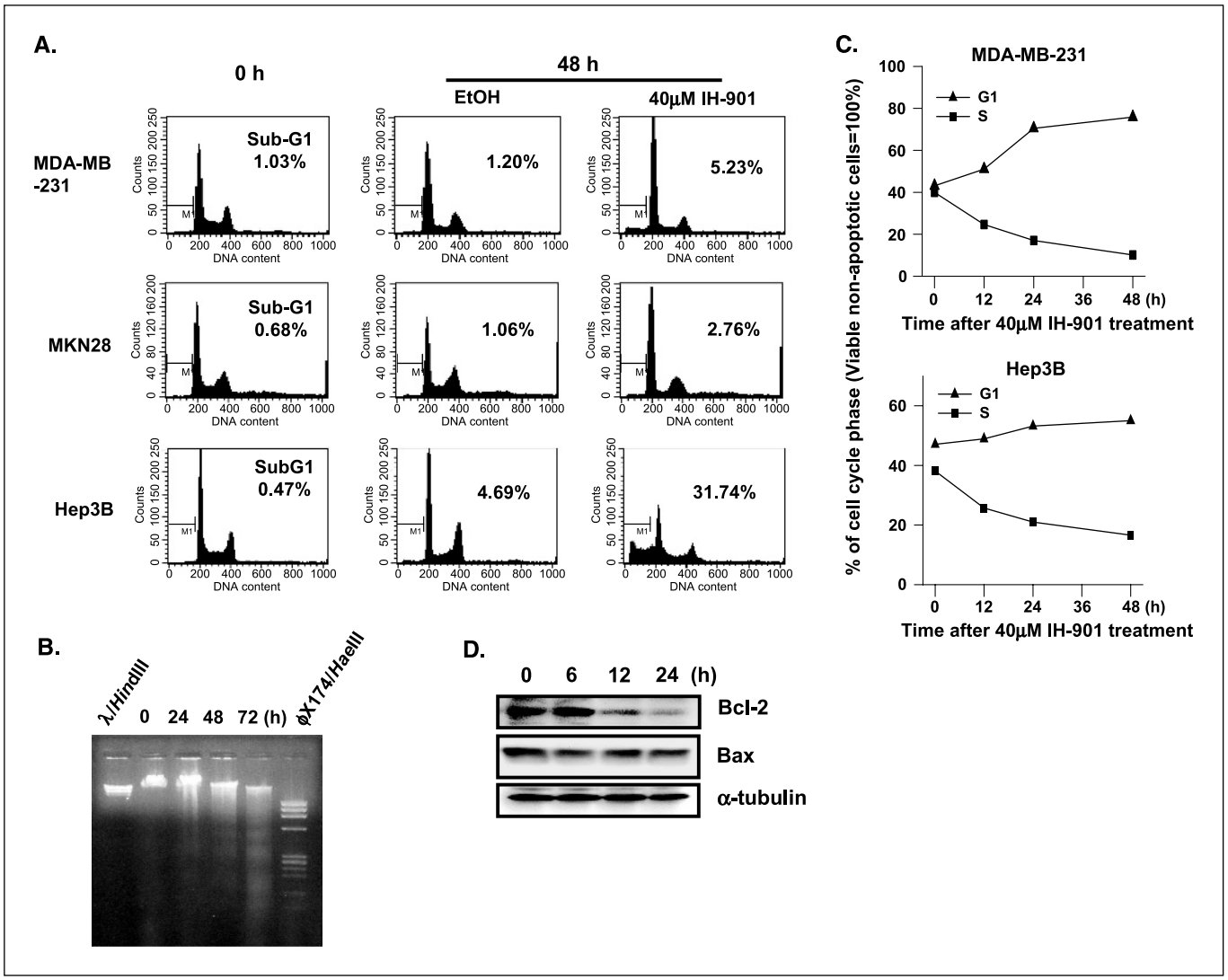

Figure 2. Cell cycle analysis of MDA-MB-231, MKN28, and Hep3B treated with 40 μmol/L IH-901 at the indicated times. After cells had been fixed and stained propidium iodide, the DNA content was measured by flow cytometry. Cell cycle distribution was analyzed using a FACStar flow cytometer (Becton Dickinson) *A,* percentages of sub-G_1 phase cells which were determined based on DNA content histogram (*inset*). *B,* induction of chromosomal DNA fragmentation by IH-901 in Hep3B cells. Chromosomal DNA was extracted from cells treated with IH-901 for the indicated times, and electrophoresed in a 1.5% agarose gel, as described in Materials and Methods. The DNA size markers, λ/*Hin*dIII and ΦX174/*Hae*III were used as controls. *C,* the population percentages of G_1 and S phase from each cell cycle phase were determined based on DNA content in (*A*) with viable nonapoptotic cells (≥2 N DNA contents). *D,* the levels of antiapoptotic Bcl-2 and proapoptotic Bax proteins were analyzed in Hep3B cells after the treatment with IH-901 for the indicated times.

siRNAs against COX-2 were controlled for sequence specificity by BLAST searching and did not show homology to other known human genes, especially COX-1. *Spe*I-*Eco*RI digested pSUPER containing U1 promoter–directed knockdown constructs were subcloned into pShuttle vector of Adeno-X Expression System (Clontech, Palo Alto, CA), thereby replacing the cytomegalovirus-promoter sequence. The sequences of the inserts and their orientations were examined by DNA sequencing analyses. siRNA expression cassettes for COX-2 or GFP from recombinant pShuttle plasmid DNA were digested and ligated to Adeno-X viral DNA according to the manufacturer's instructions. These adenoviral vectors were infected and amplified in HEK293 cells. CsCl-purified virus was dialyzed against Ca^{2+}- and Mg^{2+}-free DPBS containing 10% glycerol. The virus titer was determined using a standard plaque assay. Viral stock was aliquoted into appropriate volumes and stored at −70°C until use.

Adenovirus Infection *In vitro*. Recombinant adenoviruses expressing COX-2 or GFP siRNAs were used on the target cells at a multiplicity of infection of 20, and incubated at 37°C for 2 hours in a CO_2 incubator. The medium was removed and cells were then cultured for 24 hours before further experimentation.

Data Analysis. Results are representative of at least three independent experiments done in triplicate and are presented as mean ± SD. Comparisons between groups were analyzed using Student's paired *t* test.

Results

Effect of IH-901 on Cell Proliferation of Cancer Cells. We examined the effect of IH-901 on cellular proliferation using the 3-(4,5-dimethylthiazol-2-yl)-2,5-diphenyltetrazoliumbromide assay. Significant dose-dependent growth inhibition was observed in two breast cancer cell lines (MDA-MB-231 and Hs578T), as well as gastric (MKN28), and hepatoma (Hep3B) cell lines following treatment with IH-901 for 3 days (Fig. 1). The concentration required for 50% inhibition of growth (IC_{50}) by IH-901 ranged from 33.1 to 42.5 μmol/L. These results are consistent with earlier reports using myeloma cells

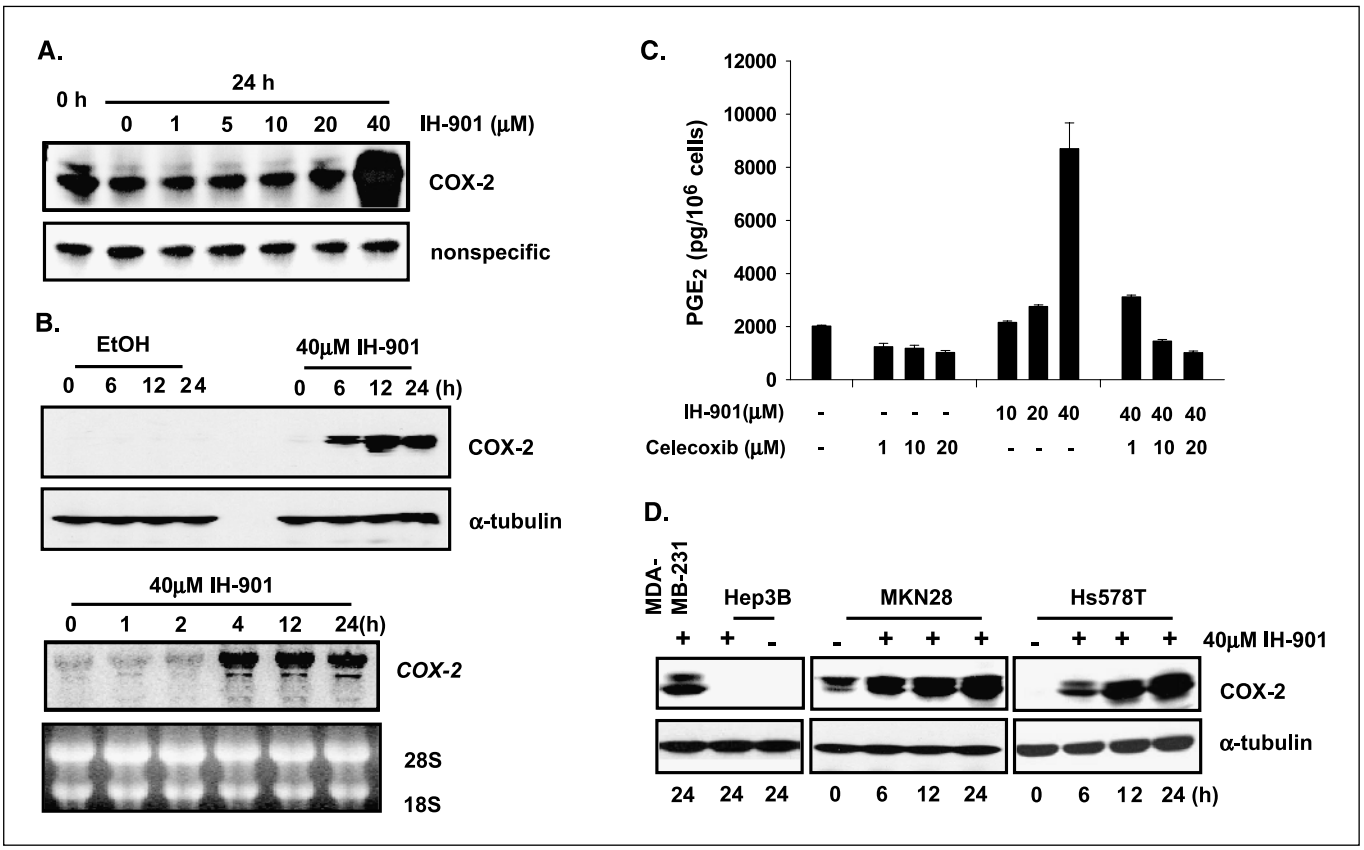

Figure 3. IH-901 induced COX-2 in MDA-MB-231, MKN28, and Hs578T cells but not in Hep3B cells. *A,* MDA-MB-231 cells were harvested after being incubated with the indicated concentrations of IH-901 for 24 hours. Equal amounts of cell extracts (100 μg/lane) were resolved by 10% SDS-PAGE and analyzed by Western blotting with an antibody specific for COX-2. *B,* treatment of MDA-MB-231 cells with 40 μmol/L IH-901 induced COX-2 expression of mRNA and protein in a time-dependent manner but vehicle (ethanol) did not. Fifteen micrograms of total RNA were used for Northern analysis. Anti-α-tubulin was used as a protein loading control. *C,* MDA-MB-231 cells were treated with varying concentrations of IH-901 and/or celecoxib for 24 hours. Conditioned media were collected and analyzed by ELISA for PGE_2. Results are expressed as the mean of six separate experiments done in duplicate. *Columns,* mean; *bars,* SD; $n = 6$. *, $P < 0.01$ compared with untreated cells. IH-901 increased PGE_2 production in a dose-dependent manner, and celecoxib effectively reduced IH-901-mediated PGE_2 production. *D,* MDA-MB-231, Hs578T, MKN28, and Hep3B cells were treated with 40 μmol/L IH-901 for 24 hours. Western analyses were done with antibodies specific to COX-2 or α-tubulin.

(8, 9). In order to examine the mechanism of growth suppression by IH-901, cancer cells were treated with 40 μmol/L IH-901 for 48 hours and then analyzed for cell cycle progression by flow cytometry. The apoptotic sub-G_1 fraction increased to 31.74% in Hep3B cells after treatment with IH-901 for 48 hours, whereas those of MDA-MB-231 and MKN28 cells were 5.23% and 2.76%, respectively, indicating that IH-901 induced a significant apoptotic cell death in Hep3B but not in MDA-MB-231 and MKN28 cells (Fig. 2*A*). The increase in the sub-G_1 fraction and endonucleolytic DNA cleavage in Hep3B cells by IH-901 was evident in a time-dependent manner (Fig. 2*B*). As shown in Fig. 2*C*, IH-901-induced cell cycle arrest at the G_0-G_1 phase and a progressive decline of S phase cells occurred in MDA-MB-231 as well as in Hep3B cells. These results suggest that IH-901 induced apoptotic cell death concurrent with cell cycle arrest in Hep3B cells, whereas it caused G_0-G_1 arrest only in MDA-MB-231 and MKN28 cells. As IH-901-mediated apoptosis is reported to be associated with the activation of caspase-3 and PARP cleavage (8, 9), levels of antiapoptotic Bcl-2 and proapoptotic Bax proteins were analyzed in Hep3B cells. Bcl-2 expression decreased in a time-dependent manner but Bax expression did not change (Fig. 2*D*). Hs578T breast cancer cell lines also showed only G_0-G_1 arrest after treatment with 40 μmol/L IH-901 (data not shown).

COX-2 Induction by Treatment with IH-901. Because several recent reports have implicated the role of COX-2 in preventing apoptosis in various cell types (19–23), we examined the ability of IH-901 to induce COX-2 in MDA-MB-231 cells. As shown in Fig. 3*A*, 40 μmol/L of IH-901 treatment resulted in the induction of COX-2 protein in MDA-MB-231 cells. COX-2 protein and mRNA were induced in a time-dependent manner by 40 μmol/L IH-901; the ethanol vehicle had no effect on COX-2 induction (Fig. 3*B*). PGE_2 production was also increased by IH-901 treatment in a dose-dependent manner, consistent with the induction of COX-2 protein (Fig. 3*C*). IH-901 also induced COX-2 protein in MKN28 and Hs578T cells but did not lead to COX-2 induction in Hep3B cells (Fig. 3*D*). Mitogen-activated protein kinase (MAPK) pathways mediate the regulation of COX-2 expression when induced by a variety of extracellular stimuli (32, 33). To determine whether IH-901 activates MAPK pathways in MDA-MB-231 cells, the levels of phosphorylated extracellular signal-regulated kinase (ERK), $p38^{MAPK}$, and c-*Jun*-NH_2-kinase proteins were evaluated by Western analysis. Western blots of MDA-MB-231 cell extracts were probed with antibodies selective for the phosphorylated (activated) forms of ERK-1 and ERK-2. As shown in Fig. 4*A*, IH-901 induced a time-dependent increase in phosphorylated ERK-1

and ERK-2 with levels elevated up to 24 hours. Marginal ethanol-induced ERK activation was also observed but this was very weak compared with IH-901-induced ERK activation (data not shown). To determine whether the activation of ERK-1 and ERK-2 is required for IH-901-mediated COX-2 induction, MDA-MB-231 cells were pretreated with UO126, a selective inhibitor of MAP/ERK kinase 1/2. UO126 (10 μmol/L) strongly inhibited IH-901-induced COX-2 expression for up to 12 hours (>Fig. 4*A*). Although blocking ERK1/2 with 10 μmol/L UO126, the cell cycle distribution of MDA-MB-231 cells was analyzed by flow cytometry (Fig. 4*B*). Cotreatment with IH-901 and UO126 caused the percentage of apoptotic sub-G_1 population to increase from 5% to 18%, compared with IH-901 treatment alone, suggesting that MAP/ERK kinase inhibition can enhance IH-901-mediated apoptosis in MAD-MB-231 cells. No significant change in the phosphorylated forms of c-jun-NH_2-kinase and $p38^{MAPK}$ was observed until 4 hours of IH-901 treatment (Fig. 4*C*).

Inhibition of COX-2 Enhances IH-901–Mediated Apoptosis. Celecoxib inhibited IH-901-induced production of PGE_2 in a dose-dependent way in MDA-MB-231 cells (Fig. 3*C*). To address whether COX-2 protein induced by IH-901 plays an important role in protecting cells from IH-901-mediated apoptosis, we examined the effects of COX-2 inhibition on IH-901-mediated apoptosis using the selective COX-2 inhibitors, celecoxib, or NS-398 (Fig. 5*A*). Briefly, MDA-MB-231 cells were treated with celecoxib (25 or 100 μmol/L) or NS-398 (100 or 500 μmol/L) for 30 minutes before adding 40 μmol/L IH-901. Cell cycle analysis showed that although celecoxib and NS-398 alone had no significant effect on the apoptotic fraction, pretreatment with celecoxib (25 μmol/L) followed by IH-901 enhanced the apoptotic sub-G_1 fraction from 5% to 40%. Similarly, NS-398 (500 μmol/L) pretreatment followed by addition of IH-901 increased the apoptotic fraction up to 30%. The combined treatment of a COX-2 inhibitor (25 μmol/L celecoxib or 200 μmol/L NS398) with 40 μmol/L IH-901 increased the apoptotic sub-G_1 fraction in Hs578T cells. These results strongly suggest that COX-2 enzyme activity protects MDA-MB-231 and Hs578T cells from IH-901-induced apoptosis. We analyzed the expression of Bcl-2 and Bax in the absence or presence of NS-398 (250 μmol/L) on 40 μmol/L IH-901 in MDA-MB-231 cells. Bcl-2 expression decreased in the presence of NS398 up to 24 hours, whereas Bax expression did not change (Fig. 5*B*). Therefore, the inhibition of COX-2 in IH-901-treated MDA-MB-231 cells changes the effect of IH-901 on the level of Bcl-2. To more specifically test the requirement for COX-2 induction in the antiapoptotic mechanism, we down-regulated the expression level of COX-2 protein by using the siRNA technique in MDA-MB-231 cells. The target sequences of siRNA used were specific for the COX-2 gene but not the COX-1 gene. We applied adenovirus-mediated delivery of siRNAs strategy to specifically reduce the expression of the COX-2 gene. The adenoviral vectors expressing siRNAs effectively reduced COX-2 gene expression, compared with parental and GFP-siRNA expressing cells, without interrupting ERK 1/2 phosphorylation following treatment with IH-901 (Fig. 5*C*). COX-2 knockdown resulted in a dramatic increase in the apoptotic sub-G_1 fraction after IH-901 treatment, compared with mock-infected and GFP knockdown (Fig. 5*D*). These results show that the COX-2 signaling pathway is critical in blocking IH-901-mediated apoptosis and that COX-2 plays an important role as an antiapoptotic molecule.

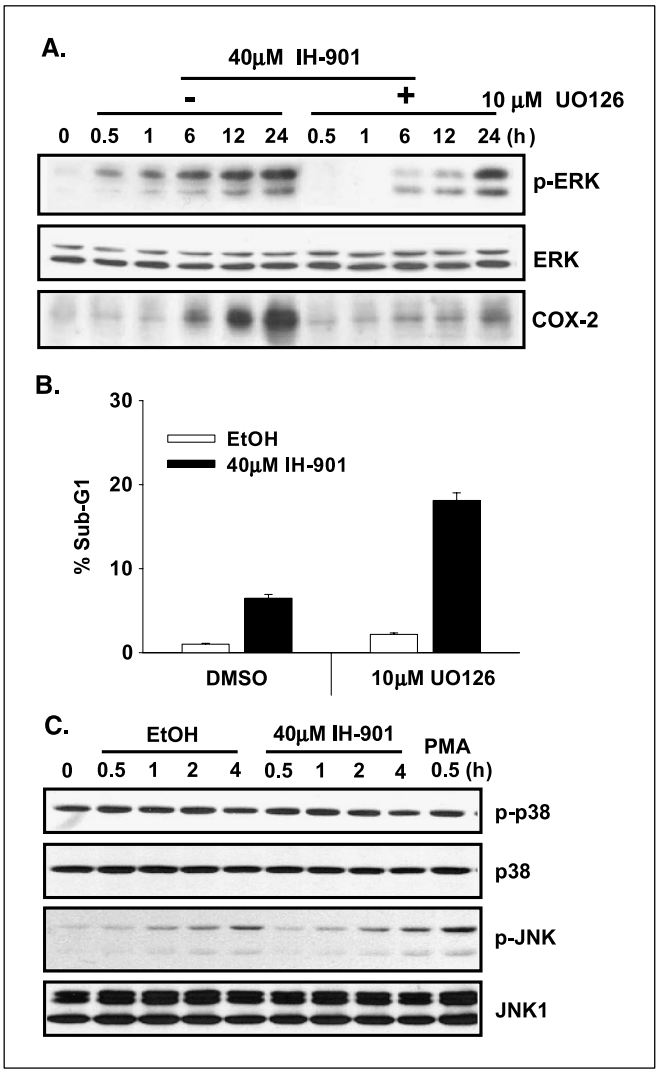

Figure 4. IH-901 induced a time-dependent increase in phosphorylated ERK1/2 in MDA-MB-231 cells. Equal amounts of cell extracts (100 μg/lane) were resolved by 10% SDS-PAGE and analyzed by Western analysis with antibodies specific to ERK1/2 or to the phosphorylated forms of ERK1/2. COX-2 induction was significantly inhibited by MAP/ERK kinase 1/2 inhibitor (UO126) in MDA-MB-231 cells. *A,* to determine whether MAPK activation is required for IH-901-induced increases in COX-2 protein levels, cells were treated with a selective MAP/ERK kinase inhibitor (UO126) 1 hour before 40 μmol/L IH-901 or vehicle addition and then incubated for 24 hours. UO126 (10 μmol/L) significantly inhibited COX-2 induction by IH-901. *B,* MDA-MB-231 cells were preincubated with 10 μmol/L UO126 for 60 minutes. Afterwards, the addition of IH-901 increased the apoptotic sub-G_1 fraction, whereas UO126 treatment alone showed no toxic effect on MDA-MB-231 cells. The percentage of sub-G_1 cells was determined based on their DNA content histograms. Representative data from three independent experiments. *C,* MDA-MB-231 cells were treated with ethanol vehicle and IH-901 for the indicated times and Western analyses of the activated form and total p38 and c-jun-NH_2-kinase expression were done. Phorbol 12-myristate 13-acetate was used for the induction of c-jun-NH_2-kinase activation.

Induction of $p27^{Kip1}$ by IH-901 Leads to the Inhibition of CDK2 Kinase Activity. Because IH-901 arrested the cell cycle at the G_0-G_1 phase in MDA-MB-231 and Hep3B cells (Fig. 2*C*), we investigated whether IH-901 affects the expressions of G_1-specific cell cycle regulatory molecules in MDA-MB-231 cells expressing mutant p53 protein (ref. 34; Fig. 6*A*). We examined the protein expression profile of cyclin-dependent kinase inhibitors associated with G_1 arrest. Western blot analysis showed that IH-901 treatment

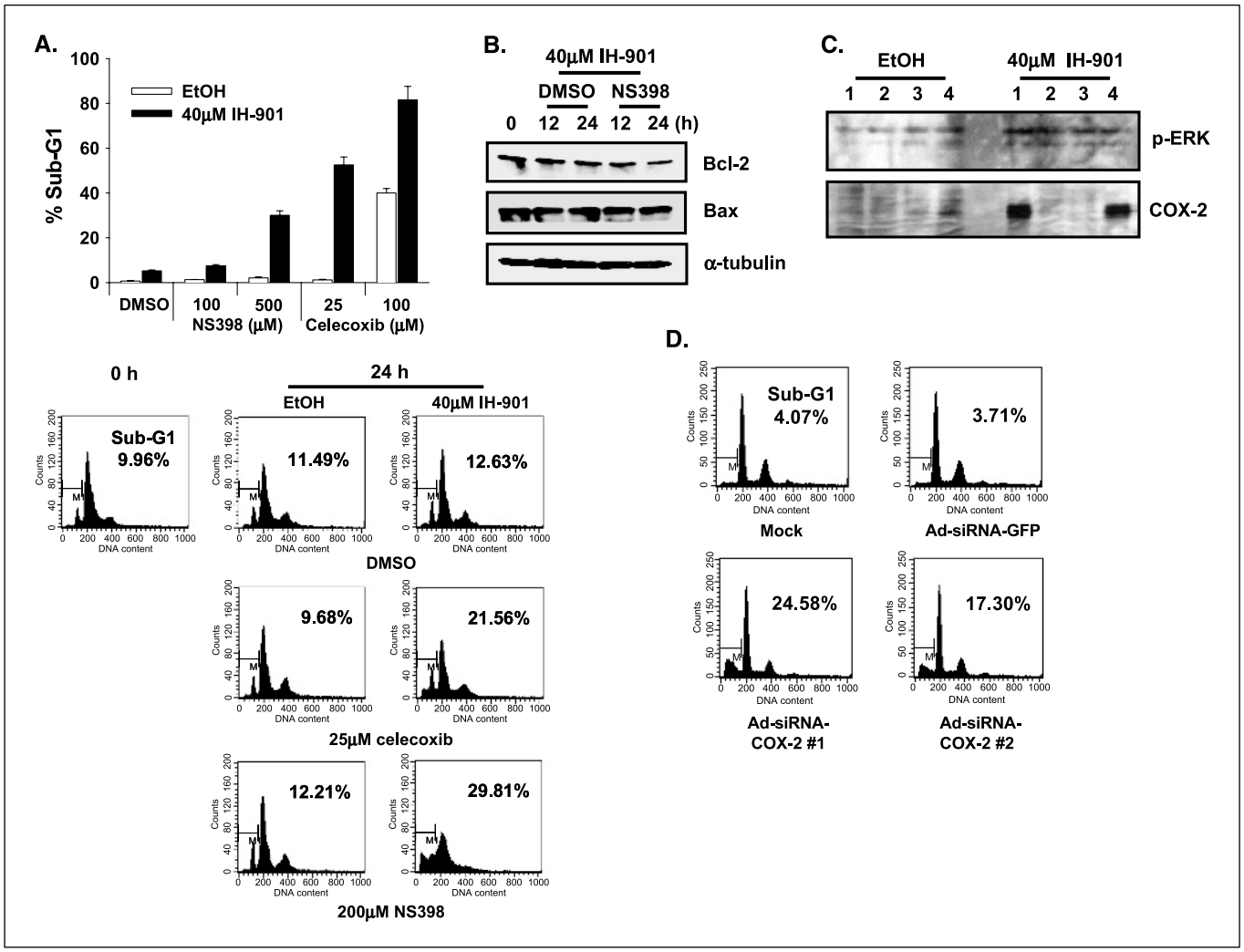

Figure 5. Inhibition of COX-2 enzyme activity or knockdown of COX-2 triggered IH-901-mediated apoptosis in MDA-MB-231 and Hs578T cells. *A,* MDA-MB-231 Cells were pretreated with NSAIDs at the indicated concentration for 30 minutes and then incubated with vehicle or 40 μmol/L IH-901 for 48 hours (*top*). Hs578T cells were pretreated with NSAIDs for 30 minutes and then incubated with vehicle or 40 μmol/L IH-901 for 24 hours (*bottom*). The population of cells in sub-G_1 phase were measured by propidium iodide staining followed by flow cytometry. Cells with <2 N of DNA content were counted as apoptotic cells and the percentages of apoptotic cells were illustrated graphically. Representative data from three independent experiments. *B,* MDA-MB-231 cells were pretreated with DMSO vehicle or 250 mmol NS398 for 30 minutes and then incubated with 40 μmol/L IH-901 for the indicated times. Western analyses were done with antibodies specific to Bcl-2, Bax, and α-tubulin. Adenoviral-mediated siRNA for COX-2 efficiently silenced COX-2 expression in MDA-MB-231 cells. After 24 hours of adenovirus-delivered siRNA infection, cells were exposed to either vehicle or 40 μmol/L IH-901 for 10 (*C*) and 24 hours (*D*). *C,* Western blot analyses were done with antibodies specific to phosphorylated forms of ERK and specific to COX-2. *Lane 1,* mock; *lane 2,* Ad-siRNA-COX-2 #1; *lane 3,* Ad-siRNA-COX-2 #2; and *lane 4,* Ad-siRNA-GFP. *D,* knockdown of COX-2 by adenoviral-mediated siRNA effectively enhanced the apoptotic fraction of IH-901 treated MDA-MB-231 cells, compared with mock-infected or GFP-siRNA-infected ones. Representative data from three independent experiments. *Inset,* percentage of sub-G_1 phase cells which was determined based on DNA content histogram.

of MDA-MB-231 cells strongly induced the protein levels of $p27^{Kip1}$ in a time-dependent manner, whereas the level of $p21^{WAF1/CIP1}$ did not change for up to 24 hours. $p16^{INK4a}$ was not detected in MDA-MB-231 or Hs578T cell lines, both of which are homozygously deleted for the *INK4* gene (35). The $p27^{Kip1}$ expression on IH-901 treatment of two cell lines, Hs578T and MKN28, showed similar pattern as in MDA-MB-231 (data not shown). Because the $p27^{Kip1}$ level was up-regulated in MDA-MB-231 cells by 40 μmol/L IH-901 within 24 hours, we investigated the effect of IH-901 on the kinase activity of CDK2 associated with cyclin E. As shown in Fig. 6*B*, treatment of MDA-MB-231 cells with IH-901 strongly decreased the histone H1-associated kinase activities of CDK2. The protein levels of cyclin D1 and cyclin E did not change for up to 48 hours after treatment (data not shown). The complexes immunoprecipitated with anti-CDK2 antibody exhibited higher amounts of $p27^{Kip1}$ from IH-901-treated MDA-MB-231 cells than from mock-treated cells. Next, we investigated the phosphorylation status of the pRb-related proteins pRb/p107 and pRb2/p130. The treatment of MDA-MB-231 cells with 40 μmol/L IH-901 increased the levels of hypophosphorylated forms of pRb and p130 in a time-dependent manner (Fig. 6*C*). SNU-16 is a control cell line used as a control for the Rb phosphorylation (27). The increase of $p27^{Kip1}$ protein levels by IH-901 resulted from the elevation of $p27^{Kip1}$ mRNA expression (Fig. 6*D*, *top*). We analyzed $p27^{Kip1}$ mRNA degradation in the absence and presence of IH-901 by Northern analysis, in actinomycin D-treated MDA-MB-231 cells (Fig. 6*D*, *bottom*). The kinetics of $p27^{Kip1}$ mRNA degradation was similar in both cases, indicating that IH-901 could induce $p27^{Kip1}$ mRNA at

the transcriptional level. The levels of $p27^{Kip1}$ were also increased in Hep3B following treatment with IH-901 (Fig. 6*A*), as observed in MDA-MB-231 cells. These results indicate that in Hep3B cells IH-901 can simultaneously induce $p27^{Kip1}$-mediated G_1 arrest as well as apoptotic cell death without COX-2 induction.

Discussion

Ginseng saponins exert various important pharmacologic effects with regard to the control of many diseases including cancer. The present study focuses on identifying the mechanism that underlies the antitumor activity of ginseng saponins. The study shows, for the first time, that IH-901, a novel ginseng saponin metabolite, can cause simultaneous growth arrest and apoptosis. Additionally, adenoviral infection of COX-2 siRNAs provides direct evidence that COX-2 protein can function as an antiapoptotic molecule.

IH-901 could induce the expression of COX-2 protein via ERK signaling. The suppression of IH-901-induced COX-2 expression by the MAP/ERK kinase inhibitor UO126 suggests that the ERK signaling pathway is important in the regulation of COX-2 by IH-901. Knockdown of COX-2 expression by siRNAs did not block ERK activation in MDA-MB-231 cells. IH-901 treatment led to the activation of ERK (data not shown) but failed to induce COX-2 in Hep3B cells. Therefore, IH-901-induced ERK activation is required but not sufficient for inhibition of apoptosis.

Several anticancer drugs have been shown to induce COX-2 expression (22, 23). For example, microtubule- or actin-interfering agents stimulate MAPK signaling and activator protein activity, enhance PGE_2 synthesis, and increase levels of COX-2 mRNA and protein (22). Epigallocatechin-3-gallate was found to up-regulate COX-2 expression and PGE_2 production in association with the activation of both the ERK and protein tyrosine phosphatase signaling pathways (36). The suppression of apoptosis by COX-2 is thought to favor carcinogenesis by permitting the survival of cells that have acquired mutations, and is viewed as one of the main mechanisms of tumorigenesis. As COX-2 induction by anticancer drugs may result in unwanted effects such as inflammation, the combined use of selective COX-2 inhibitors and conventional anticancer drugs has been suggested (23).

However, the interpretation of previous NSAID studies was complicated by possible COX-independent mechanisms. In many cases, NSAIDs alone induced apoptosis at much higher concentrations than their IC_{50}'s. COX-2 mutant proteins lacking COX activity have been reported to inhibit cell cycle progression in a variety of cell types (37). In order to confirm that COX-2 protein is an antiapoptotic molecule, we constructed adenoviral COX-2 siRNAs for selective targeting of the COX-2 protein itself rather than opting to use NSAIDs to inhibit COX-2 enzymatic activity. Our data shows that both NSAID treatment and knock-down of the COX-2 gene by siRNAs could cause apoptosis

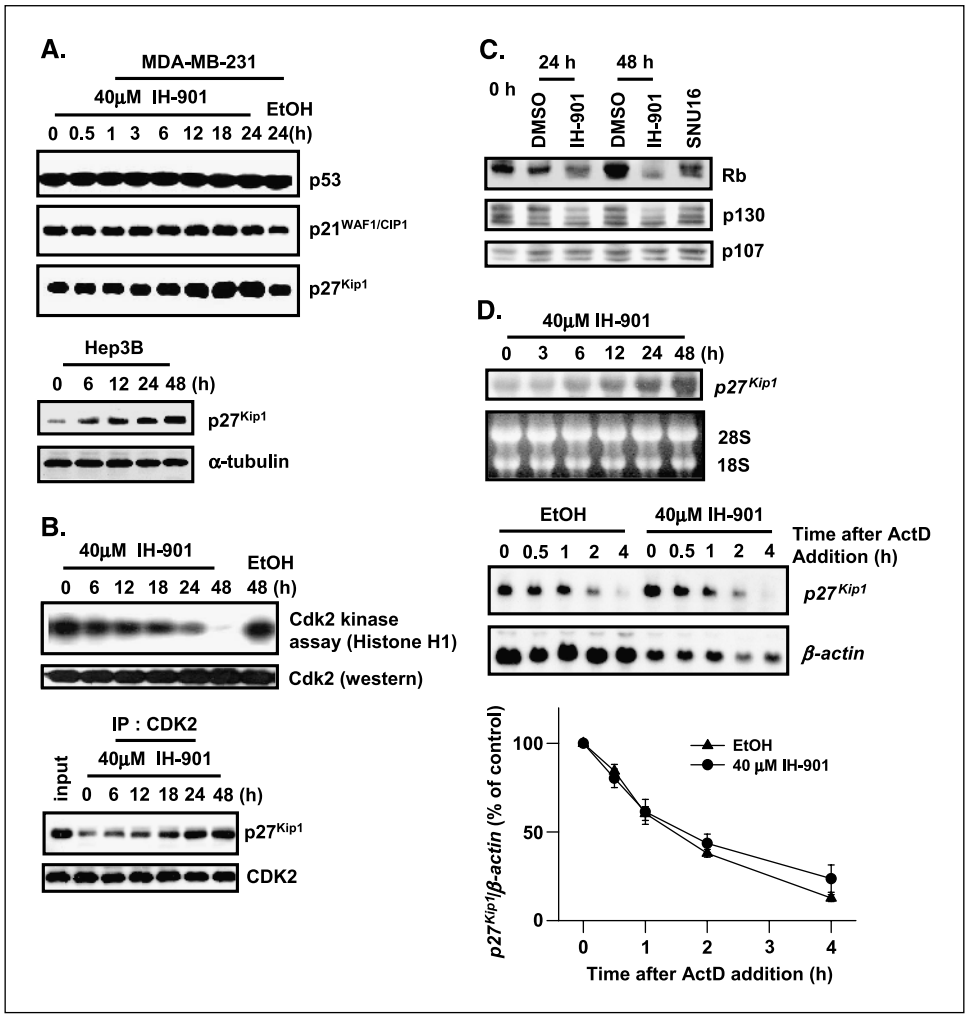

Figure 6. Effect of G_1 phase-associated regulatory proteins in MDA-MB-231 cells treated with IH-901. MDA-MB-231 cells were treated with vehicle (ethanol) or 40 μmol/L IH-901 for the indicated times. Cell lysates (30 μg of protein per lane) were resolved by SDS-PAGE, and proteins were detected by immunoblotting with antibodies against the indicated molecules. *A,* Western blot analysis showed that IH-901 treatment of MDA-MB-231 (*top*) and Hep3B (*bottom*) induced the protein levels of $p27^{Kip1}$. *B,* IH-901 treatment of MDA-MB-231 cells strongly decreased the histone H1-associated kinase activities of CDK2 in a time-dependent manner (*top*). The complexes immunoprecipitated with anti-CDK2 antibody exhibited higher amounts of immunodetectable $p27^{Kip1}$ protein from IH-901-treated cells in a time dependent manner (*bottom*). *C,* IH-901 increased hypophosphorylated levels of pRb and p130. SNU-16 is a gastric cancer cell line used as a control for the Rb phosphorylation (27). *D,* IH-901 treatment elevated the mRNA expression of $p27^{Kip1}$ (*top*). $p27^{Kip1}$ mRNA stability assay (*bottom*). MDA-MB-231 cells were treated with 40 μmol/L IH-901 for 22 hours, followed by addition of 10 μg/mL actinomycin D at time 0. At the indicated time intervals, total RNAs were isolated and Northern analysis was done. Graph shows the remaining $p27^{Kip1}$ mRNA quantified after being normalized to corresponding amounts of β-*actin* mRNA. *Points,* mean of three separate experiments in duplicate; *bars,* ± SE.

in MDA-MB-231 cells, providing direct evidence that COX-2 protein plays an important role in suppressing IH-901-mediated apoptosis.

Thus far, the antitumor activity of IH-901 has been attributed solely to apoptosis (8, 9). However, in this study, we show a second mechanism: cell cycle arrest. IH-901 strongly induced $p27^{Kip1}$ and inhibited CDK2 activities followed by an increase in hypophosphorylated levels of pRb and p130. These molecular effects of IH-901, especially the up-regulation of $p27^{Kip1}$, may play important roles in the G_1 arrest seen in MDA-MB-231, MKN28, Hs578T, and Hep3B cells. The observed up-regulation of $p27^{Kip1}$ by IH-901 and resulting decrease of CDK2 kinase activity is important and consistent with an earlier report that decreased $p27^{Kip1}$ expression in breast carcinomas are associated with aggressive phenotypes and that adenoviral infection with human $p27^{Kip1}$ resulted in cell cycle arrest (38). The pRb-related proteins, p107 and p130, cooperate to regulate cell cycle progression at G_1-S checkpoint. It has been reported that p130 and $p27^{Kip1}$ are mutually involved in the negative regulation of cellular proliferation (39). IH-901 reduced CDK2-cyclin E kinase activity, and increased the hypophosphorylated levels of Rb-related proteins. Hep3B is known to be Rb-negative (40) and has mutant p53 (41). Even though Hep3B cells showed marginal G_1 arrest, the progressive decline of the S phase was indicative of G_1 arrest (Fig. 2*C*). However, it is difficult to exclude the possibility of the involvement of $p21^{WAF1/CIP1}$ in IH-901-mediated growth arrest because all four cell lines used in this study express mutant p53. We found the induction of $p21^{WAF1/CIP1}$ mRNA and protein in a carcinoma cell line containing wild-type p53 after the treatment with IH-901 (data not shown). Collectively, the growth inhibitory effects of IH-901 in cells could be caused by the following progression: induction of $p27^{Kip1}$ leads to a decrease in kinase activity of CDKs followed by modulation of further downstream targets such as pRb-related proteins and the E2F family of transcription factors family.

In summary, the findings of this study show that IH-901, a novel ginseng saponin metabolite, induces apoptosis and inhibits cell proliferation by G_1 arrest via increase of $p27^{Kip1}$ expression. COX-2 induction caused by IH-901 could diminish the antitumor effects, and strongly suggests the therapeutic use of COX-2 siRNAs to inhibit COX-2. Further study will contribute to the development of IH-901 or ginseng-related drugs as potential chemotherapeutic or chemopreventive agents.

Acknowledgments

Received 5/18/2004; revised 11/16/2004; accepted 12/29/2004.

Grant support: Supported in part by the National Cancer Control R&D Program 2003, Ministry of Health and Welfare, Republic of Korea; by Seoul National University Cancer Research Institute; and by the 2002 BK21 Project for Medicine, Dentistry, and Pharmacy.

The costs of publication of this article were defrayed in part by the payment of page charges. This article must therefore be hereby marked advertisement in accordance with 18 U.S.C. Section 1734 solely to indicate this fact.

We thank the Il Hwa Company for providing IH-901, Drs. S.M. Prescott for cDNA construct of COX-2 and J-W. Soh for his helpful discussion, and to J.S. Koh for his critical editing of this manuscript.

References

1. Yun TK. Experimental and epidemiological evidence on non-organ specific cancer preventive effect of Korean ginseng and identification of active compounds. Mutat Res 2003;523-524:63–74.
2. Yun TK, Choi SY, Yun HY. Epidemiological study on cancer prevention by ginseng: are all kinds of cancers preventable by ginseng? J Korean Med Sci 2001;16 Suppl:S19–27.
3. Shin HR, Kim JY, Yun TK, Morgan G, Vainio H. The cancer-preventive potential of *Panax ginseng*: a review of human and experimental evidence. Cancer Causes Control 2000;11:565–76.
4. Hasegawa H, Sung JH, Matsumiya S, Uchiyama M. Main ginseng saponin metabolites formed by intestinal bacteria. Planta Med 1996;62:453–7.
5. Hasegawa H, Sung JH, Matsumiya S, et al. Reversal of daunomycin and vinblastine resistance in multidrug-resistant P388 leukemia *in vitro* through enhanced cytotoxicity by triterpenoids. Planta Med 1995;61:409–13.
6. Lee SJ, Sung JH, Lee SJ, Moon CK, Lee BH. Antitumor activity of a novel ginseng saponin metabolite in human pulmonary adenocarcinoma cells resistant to cisplatin. Cancer Lett 1999;144:339–43.
7. Lee BH, Lee SJ, Hur JH, et al. *In vitro* antigenotoxic activity of novel ginseng saponin metabolites formed by intestinal bacteria. Planta Med 1998;64:500–3.
8. Lee SJ, Ko WG, Kim JH, Sung JH, Moon CK, Lee BH. Induction of apoptosis by a novel intestinal metabolite of ginseng saponin via cytochrome *c*-mediated activation of caspase-3 protease. Biochem Pharmacol 2000;60: 677–85.
9. Choi HH, Jong HS, Park JH, et al. A novel ginseng saponin metabolite induces apoptosis and down-regulates fibroblast growth factor receptor 3 in myeloma cells. Int J Oncol 2003;23:1087–93.
10. Subbaramaiah K, Dannenberg AJ. Cyclooxygenase 2: a molecular target for cancer prevention and treatment. Trends Pharmacol Sci 2003;24:96–102.
11. Wang D, Dubois RN. Cyclooxygenase-2: a potential target in breast cancer. Semin Oncol 2004;31:64–73.
12. Eberhart CE, Coffey RJ, Radhika A, Giardiello FM, Ferrenbach S, DuBois RN. Up-regulation of cyclooxygenase 2 gene expression in human colorectal adenomas and adenocarcinomas. Gastroenterology 1994;107:1183–8.
13. Lim HY, Joo HJ, Choi JH, et al. Increased expression of cyclooxygenase-2 protein in human gastric carcinoma. Clin Cancer Res 2000:6:519–25.
14. Shim V, Gauthier ML, Sudilovsky D, et al. Cyclooxygenase-2 expression is related to nuclear grade in ductal carcinoma *in situ* and is increased in its normal adjacent epithelium. Cancer Res 2003;63:2347–50.
15. Yoshimatsu K, Altorki NK, Golijanin D, et al. Inducible prostaglandin E synthase is overexpressed in non-small cell lung cancer. Clin Cancer Res 2001;7:2669–74.
16. Fujita H, Koshida K, Keller ET, et al. Cyclooxygenase-2 promotes prostate cancer progression. Prostate 2002;53:232–40.
17. Chang SH, Liu CH, Conway R, et al. Role of prostaglandin E_2-dependent angiogenic switch in cyclooxygenase 2-induced breast cancer progression. Proc Natl Acad Sci U S A 2004;101:591–6.
18. Pai R, Nakamura T, Moon WS, Tarnawski AS. Prostaglandins promote colon cancer cell invasion; signaling by cross-talk between two distinct growth factor receptors. FASEB J 2003;17:1640–7.
19. Cao Y, Prescott SM. Many actions of cyclooxygenase-2 in cellular dynamics and in cancer. J Cell Physiol 2002;190:279–86.
20. Nzeako UC, Guicciardi ME, Yoon JH, Bronk SF, Gores GJ. COX-2 inhibits Fas-mediated apoptosis in cholangiocarcinoma cells. Hepatology 2002;35:552–9.
21. Sun Y, Tang XM, Half E, Kuo MT, Sinicrope FA. Cyclooxygenase-2 overexpression reduces apoptotic susceptibility by inhibiting the cytochrome *c*-dependent apoptotic pathway in human colon cancer cells. Cancer Res 2002;62:6323–8.
22. Subbaramaiah K, Hart JC, Norton L, Dannenberg AJ. Microtubule-interfering agents stimulate the transcription of cyclooxygenase-2. Evidence for involvement of ERK1/2 AND p38 mitogen-activated protein kinase pathways. J Biol Chem 2000;275: 14838–45.
23. Hsueh CT, Chiu CF, Kelsen DP, Schwartz GK. Selective inhibition of cyclooxygenase-2 enhances anticancer drug-induced apoptosis. Cancer Chemother Pharmacol 2000;45:389–96.
24. Milas L, Hanson WR. Eicosanoids and radiation. Eur J Cancer 1995;31A:1580–5.
25. Polyak K, Kato JY, Solomon MJ, et al. $p27^{Kip1}$, a cyclin-Cdk inhibitor, links transforming growth factor-β and contact inhibition to cell cycle arrest. Genes Dev 1994;8:9–22.
26. Rao S, Gray-Bablin J, Herliczek TW, Keyomarsi K. The biphasic induction of p21 and p27 in breast cancer cells by modulators of cAMP is posttranscriptionally regulated and independent of the PKA pathway. Exp Cell Res 1999;252:211–23.
27. Kim SG, Kim SN, Jong HS, et al. Caspase-mediated Cdk2 activation is a critical step to execute transforming growth factor-β1-induced apoptosis in human gastric cancer cells. Oncogene 2001;20:1254–65.
28. Jong HS, Lee HS, Kim TY, et al. Attenuation of transforming growth factor β-induced growth inhibition in human hepatocellular carcinoma cell lines by cyclin D1 overexpression. Biochem Biophys Res Commun 2002;292:383–9.
29. Kim SG, Jong HS, Kim TY, et al. Transforming growth factor-β1 induces apoptosis through Fas ligand-independent activation of the Fas death pathway in human gastric SNU-620 carcinoma cells. Mol Biol Cell 2004;15:420–34.
30. Song SH, Jong HS, Choi HH, et al. Transcriptional silencing of cyclooxygenase-2 by hypermethylation of the 5′ CpG island in human gastric carcinoma cells. Cancer Res 2001;61:4628–35.
31. Brummelkamp TR, Bernards R, Agami R. A system for stable expression of short interfering RNAs in mammalian cells. Science 2002;296:550–3.
32. Saha D, Datta PK, Sheng H, et al. Synergistic induction of cyclooxygenase-2 by transforming growth factor-β1 and epidermal growth factor inhibits apoptosis in epithelial cells. Neoplasia 1999;1:508–17.
33. Fan XM, Wong BC, Lin MC, et al. Interleukin-1β induces cyclo-oxygenase-2 expression in gastric cancer

cells by the p38 and p44/42 mitogen-activated protein kinase signaling pathways. J Gastroenterol Hepatol 2001;16:1098–104.
34. Negrini M, Sabbioni S, Haldar S, et al. Tumor and growth suppression of breast cancer cells by chromosome 17-associated functions. Cancer Res 1994;54:1818–24.
35. Musgrove EA, Lilischkis R, Cornish AL, et al. Expression of the cyclin-dependent kinase inhibitors $p16^{INK4}$, $p15^{INK4B}$ and $p21^{WAF1/CIP1}$ in human breast cancer. Int J Cancer 1995;63:584–91.
36. Park JW, Choi YJ, Suh SI, Kwon TK. Involvement of ERK and protein tyrosine phosphatase signaling pathways in EGCG-induced cyclooxygenase-2 expression in Raw 264.7 cells. Biochem Biophys Res Commun 2001;286:721–5.
37. Trifan OC, Smith RM, Thompson BD, Hla T. Overexpression of cyclooxygenase-2 induces cell cycle arrest. Evidence for a prostaglandin-independent mechanism. J Biol Chem 1999;274:34141–7.
38. Craig C, Wersto R, Kim M, et al. A recombinant adenovirus expressing $p27^{KIP1}$ induces cell cycle arrest and loss of cyclin-Cdk activity inhuman breast cancer cells. Oncogene 1997;14:2283–9.
39. Howard CM, Claudio PP, De Luca A, et al. Inducible pRb2/p130 expression and growth-suppressive mechanisms:evidenceofapRb2/p130,$p27^{KIP1}$,and cyclin E negative feedback regulatory loop. Cancer Res 2000;60:2737–44.
40. Hashimoto O, Ueno T, Kimura R, et al. Inhibition of proteasome-dependent degradation of Wee1 in G_2-arrested Hep3B cells by TGF-β1. Mol Carcinog 2003;36:171–82.
41. Lin Y, Shi CY, Li B, et al. Tumour suppressor p53 and Rb genes in human hepatocellular carcinoma. Ann Acad Med Singapore 1996;25:22–30.

Cyclooxygenase-2 Inhibits Novel Ginseng Metabolite-Mediated Apoptosis

Hyung Woo Yim, Hyun-Soon Jong, Tai Young Kim, et al.

Cancer Res 2005;65:1952-1960.